

Modeling of Hydrogen Production from Bio-Oil via Steam Reforming using Matlab

By

Mohd Zharif Bin Imrat

A project dissertation submitted to the
Chemical Engineering Programme
Universiti Teknologi PETRONAS
In partial fulfillment of the requirement for the
Bachelor of Engineering (Hons)
(Chemical Engineering)

January 2009

Universiti Teknologi PETRONAS
Bandar Seri Iskandar
31750 Tronoh
Perak Darul Ridzuan

CERTIFICATION OF APPROVAL

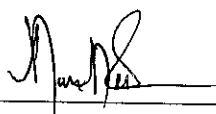
MODELING OF HYDROGEN PRODUCTION FROM BIO OIL VIA STEAM REFORMING USING MATLAB

By

Mohd Zharif Bin Imrat

A project dissertation submitted to the
Chemical Engineering Programme
Universiti Teknologi PETRONAS
In partial fulfillment of the requirement for the
BACHELOR OF ENGINEERING (Hons)
(CHEMICAL ENGINEERING)

Approved by,



(Dr. Murni Melati Ahmad)

UNIVERSITI TEKNOLOGI PETRONAS
TRONOH, PERAK
JANUARY 2006

CERTIFICATION OF ORIGINALITY

This is to certify that I am responsible for the work submitted in this project, that the original work is my own except as specified in the reference and acknowledgement, and that the original work contained herein have not been undertaken or done by unspecified sources or persons.



MOHD ZHARIF BIN IMRAT

ABSTRACT

Biomass is a product in which is a renewable resource that can be used for production of hydrogen. The hydrogen has the potential to be a source for alternative fuel required in the future. The alternative way concept is based on a two-stage process, which are fast pyrolysis and catalytic steam reforming [17]. There exists a wide range of modeling approaches to represent hydrogen production from bio oil via steam reforming. The modeling approach, even it is less expensive and more extendable compared to experimental procedures, has its own limitation. In this project, the bio oil will be represented by crude ethanol as there are difficulties of finding the right journals. The main objective for this project is to screen suitable models to represent hydrogen production from bio-oil via steam reforming. The models of each process steps in hydrogen production are compiled by MATLAB. The process steps from steam reforming to water gas shift reaction, to PSA purification of hydrogen are gathered into one system so that the integrated results can be determined. In the case of steam reforming process, Model 1 has the Average Relative Error of 29.1%. Whereas for Model 2 and Power Law, both have the Average Relative Error of 21.1% and 17.2% respectively. Basically, Model 2 and Power Law are on the active site of the Rate Determining Step as the Average Relative Error is less than 25 %. For the Water Gas Shift reaction, it is concluded that the final temperature for the shift reactor for this system is around 493 K. The conversion of the reactor is 68 % and the GHSV will be approximately about 6250 h^{-1} . Finally, the H_2 purity for this work is 98.9119 % because the bed only consists of activated carbon with the purpose is to trap CO_2 . It is determined that the Relative error (%) for this work and Ribeiro ., based on H_2 purity is 1.08 %.

ACKNOWLEDGEMENT

First and foremost, I would like to thank to God Almighty, Allah for giving an opportunity to perform this Final Year Project in such a great manner. Greatest appreciation also to my beloved family for being well supportive, which really helps me to complete this project.

Special thanks also to Dr. Murni Melati, who is a project supervisor for providing excellent help, guidance, patience and willingness to share out her knowledge and experience in order for me to complete the project. Endless thanks and appreciation to friends for their ideas in bringing this project to success. Their kindness and friendliness will never be forgotten. Their contribution will be remembered and only God can repay their kindness. Thank you very much.

TABLE OF CONTENT

<i>CERTIFICATION OF APPROVAL</i>	1
<i>CERTIFICATION OF ORIGINALITY</i>	2
<i>ABSTRACT</i>	3
<i>ACKNOWLEDGEMENT</i>	4
<i>TABLE OF CONTENT</i>	5
<i>LIST OF FIGURES</i>	7
<i>LIST OF FIGURES</i>	8
<i>CHAPTER 1: INTRODUCTION</i>	10
1.1 BACKGROUND	10
1.2 CONCEPTS	11
1.2.2 <i>Pyrolysis Process</i>	11
1.2.3 <i>Steam Reforming</i>	12
1.2.4 <i>Water Gas Shift Reaction</i>	12
1.3 CHEMICAL REACTION ANALYSIS	14
1.4 PROCESS FLOW DIAGRAM	15
1.5 PROBLEM STATEMENT	17
1.6 OBJECTIVE	18
<i>CHAPTER 2: LITERATURE REVIEW</i>	19
2.1 STEAM REFORMING	19
2.2 WATER GAS SHIFT REACTION	21
2.3 HYDROGEN PURIFICATION	22
<i>CHAPTER 3: METHODOLOGY</i>	24
3.1 OVERVIEW OF OVERALL PROJECT METHODOLOGY	24
3.2 PROJECT GANT CHART	26
3.3 PROCESS DEVELOPMENT	26

<i>CHAPTER 4: RESULTS AND DISCUSSION</i>	28
4.1 STEAM REFORMING OF CRUDE ETHANOL	28
4.1.1 <i>The calculation of rate of reaction</i>	28
4.1.2 <i>The calculation of Component Balance</i>	37
4.2 WATER GAS SHIFT REACTION.....	40
4.2.1 <i>The calculation of rate of reaction</i>	40
4.2.2 <i>The calculation of Component Balance</i>	45
4.3 HYDROGEN PURIFICATION (PSA PURIFICATION)	47
4.3.1 <i>The calculation of Component Balance</i>	47
<i>CHAPTER 5: CONCLUSION</i>	53
<i>REFERENCES</i>	54
<i>APPENDICES</i>	57
APPENDIX 1: OPERATING UNIT DESCRIPTION.....	57
APPENDIX 2: PROJECT GANT CHART FYP 1	59
APPENDIX 3: PROJECT GANT CHART FYP 2	60
APPENDIX 4: STEAM_REFORMING_MODEL1.M.....	61
APPENDIX 5: STEAM_REFORMING_MODEL2.M.....	63
APPENDIX 6: POWER_LAW_MODEL.M	65
APPENDIX 7: WGS-NUMEC_FIT.M	66

LIST OF FIGURES

<i>Figure 1.1:</i>	<i>Simplified Process Flow Diagram</i>	15
<i>Figure 1.2:</i>	<i>Process flow diagram of the bio-oil reforming</i>	16
<i>Figure 3.1:</i>	<i>Block Diagram of Project Methodology</i>	24
<i>Figure 3.2:</i>	<i>Block Diagram Each Step Process in Hydrogen Production from Ethanol</i>	26
<i>Figure 4.1:</i>	<i>Variation of crude ethanol conversion with space time</i>	28
<i>Figure 4.2:</i>	<i>A comparison of measured and predicted rates of reforming crude ethanol within the temperature Range of 593-793 K</i>	33
<i>Figure 4.3:</i>	<i>Water Gas Shift Reaction - CO conversion as a function of space velocity</i>	41
<i>Figure 4.4:</i>	<i>Graph of molar flowrate for H₂ along the bed from 0 m to 0.5 m at 80,000s</i>	50
<i>Figure 4.5:</i>	<i>Graph of molar flowrate for CO₂ along the bed from 0 m to 0.5 m at 80,000 s</i>	51

LIST OF FIGURES

<i>Table 1.1:</i>	<i>Crude Ethanol Composition</i>	17
<i>Table 4.1:</i>	<i>Value of slopes (predicted r_A) at temperature 593, 693, 793 K</i>	30
<i>Table 4.2:</i>	<i>Table of kinetic models</i>	30
<i>Table 4.3:</i>	<i>Nomenclature for catalytic reforming of crude ethanol</i>	31
<i>Table 4.4:</i>	<i>Kinetic experimental data for catalytic reforming of crude ethanol</i>	32
<i>Table 4.5:</i>	<i>Fitted values of kinetic constants of crude ethanol reforming to hydrogen based on model 1, model 2 and power law</i>	32
<i>Table 4.6:</i>	<i>The values of the measured r_A for the three models along with the predicted r_A.</i>	33
<i>Table 4.7:</i>	<i>Model 1 average relative error</i>	34
<i>Table 4.8:</i>	<i>Model 2 average relative error</i>	34
<i>Table 4.9:</i>	<i>Power Model average relative error</i>	35

<i>Table 4.10:</i>	<i>Calculated Average for each Temperature for Power Law Model</i>	35
<i>Table 4.11:</i>	<i>Conversion, X of Calculated Average for each Temperature for Power Law Model</i>	36
<i>Table 4.12:</i>	<i>Value of slopes (predicted r_{CO}) at temperature 428, 463, 493 K</i>	42
<i>Table 4.13:</i>	<i>Conversion, X of r_{CO} for each Temperature for empirical rate expression derieved from the numerical fitting</i>	44
<i>Table 4.14:</i>	<i>Calculated molar flowrates for H₂ and CO₂ along the bed from 0 m to 0.5 m at t=80,000 s</i>	50

CHAPTER 1: INTRODUCTION

1.1 Background

Due to the rising price of fossil fuel in the global market, along with the increasing in energy consumption and demand, exploration of alternative and renewable resource of energy has been developed. Together with the depleted source of fossil fuel and the awareness of the environment since 1990s, which is the significant global warming trend, has lead to the exploration of a new alternative energy resource such as hydrogen. This resource is becoming popular alternative in order to replace other energy resources especially for transportation fuel and power generation, while maintaining the sustainable, economically viable and eco-friendly source.

Hydrogen production from renewable resources, such as biomass, is gaining attention since the use of biomass for energy does not increase carbon dioxide emissions. It also does not contribute to the risk of global climate change, as it is particularly a clean resource. One of the common processes to produce hydrogen from biomass is via fast pyrolysis of biomass into bio-oil and steam reforming of bio-oil into hydrogen. The hydrogen yield from the bio-oil can be further increased via water gas shift reaction. The combination of fast pyrolysis of biomass followed by steam reforming of the produced bio-oil has attracted attention of the research community [1-3], as one of the most promising methods for hydrogen production.

Bio-oil has certain advantages such as higher density than biomass, easy storage and transportation, easy to be used either as a renewable liquid fuel or for the production of chemicals. By addition, bio oil can be separated into a hydrophobic lignin derived fraction and an aqueous fraction (50% of bio-oil) containing mostly carbohydrate derived monomeric compounds [4,5]. The aqueous phase of the bio-oil consists of 20% organics and 80% water [6-8].

1.2 Concepts

1.2.2 Pyrolysis Process

Pyrolysis is a chemical decomposition of organic materials by heating in the absence of oxygen or any other reagents, except steam. It is used in chemical analysis to break down complex matter into simpler molecules for identification. In industry, it is used to convert one single chemical to multiple chemicals. For instance, ethylene dichloride is pyrolysed to vinyl chloride in order to make PVC. It is also used to convert complex materials to substances that are less harmful such as biomass or waste. Extreme pyrolysis can also be called as carbonization, as it leaves only carbon as the residue.

Fast pyrolysis of biomass feedstocks is required to achieve high yields of liquids. It is characterized by rapid heating of the biomass particles and a short residence time of product vapors (0.5 to 2 s). Rapid heating is where the biomass is grounded into fine particles and the insulating char layer that forms at the surface of the reacting particles must be removed continuously. Since pyrolysis is endothermic, various methods have been proposed in order to provide heat to the reacting biomass particles:

- Partial combustion of the biomass products through air injection. This will result in poor-quality products.
- Direct heat transfer with a hot gas, ideally product gas that is reheated and recycled. The problem is to provide enough heat with reasonable gas flow-rates.
- Indirect heat transfer with exchange surfaces (wall, tubes). It is difficult to achieve good heat transfer on both sides of the heat exchange surface.
- Direct heat transfer with circulating solids: Solids transfer heat between a burner and a pyrolysis reactor. This is an effective but complex technology.

There are a lot of technologies that have been proposed for the biomass pyrolysis process. But, for this project, only two of those technologies will be emphasized. The following technologies that have been proposed for the biomass pyrolysis process:

- Fixed beds: For the traditional production of charcoal, bulk catalysts are used. But, the consequence of using this technology is a poor and slow heat transfer will result in very low liquid yields.
- Fluidized beds: Biomass particles are introduced into a bed of hot sand fluidized by a gas, which is usually a recirculated product gas. Biomass particles experience a rapid heating because of high heat transfer rates from fluidized sand. There is some ablation by attrition with the sand particles, but it is not as effective as in the ablative processes. Heat exchanger tubes will provide heat through which hot combustion gas flows. There will be some dilution of the products, which will make it difficult to condense.

1.2.3 Steam Reforming

Steam reforming (SR), hydrogen reforming or catalytic oxidation, is a method of producing hydrogen from hydrocarbons. It is a dominant method for producing hydrogen in industrial scale.

Steam reforming of natural gas or syngas is the most common method of producing commercial bulk hydrogen as well as the hydrogen used in the industrial synthesis of ammonia. It is also the least expensive method. At high temperatures (700 – 1100 °C) and in the presence of a metal-based catalyst (nickel), steam reacts with methane to yield carbon monoxide and hydrogen. This steam reforming process is quite different and not to be confused with catalytic reforming of naphtha, an oil refinery process that also produces significant amounts of hydrogen along with high octane gasoline.

1.2.4 Water Gas Shift Reaction

The water-gas shift reaction (WGS) is a chemical reaction in which carbon monoxide reacts with water to form carbon dioxide and hydrogen. The water-gas shift reaction is an exothermic and also important industrial reaction.

The water gas shift reaction is sensitive to temperature, with the tendency to shift towards reactants as temperature increases due to Le Chatelier's principle. In fuel-rich hydrocarbon combustion processes, the water gas reaction at equilibrium state is often employed as a means to provide estimates for molar concentrations of burnt gas constituents.

The process is used in two stages, stage one a high temperature shift (HTS) at 350 °C (662 °F) and stage two a low temperature shift (LTS) at 190-210 °C (374-410 °F). Standard industrial catalysts for this process are iron oxide promoted with chromium oxide for the HTS step and copper on a mixed support composed of zinc oxide and aluminum oxide for the LTS shift step. Attempts to lower the reaction temperature of this reaction have been done primarily with a catalyst such as Fe_3O_4 (magnetite), or other transition metals and transition metal oxides.

1.3 Chemical Reaction Analysis

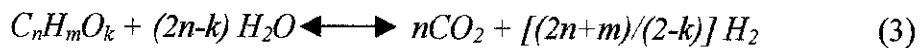
According to Rioche et al. [15], the steam reforming of bio-oil oxygenated organic compounds with chemical formula $C_nH_mO_k$ is described as follows:



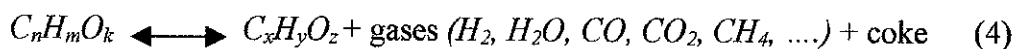
The reaction is followed by water gas shift reaction (WGS):



The steam reforming reaction is endothermic (+ve), thus favoring high temperatures while the carbon monoxide shift reaction is exothermic (-ve). The overall reforming process given that both the reactions above can be represented as follows:



Due to high temperature of the reaction, thermal decomposition or cracking can occur which causes coke and a mixture of gases such as hydrogen, carbon monoxide, carbon dioxide, methane, and carbon to be formed. The detail reaction is represented as follows:



Due to the formation of the two undesirable products, carbon monoxide and methane, which are formed during WGS and methanation reaction, the actual yield of hydrogen is lower than the stoichiometric maximum.

1.4 Process Flow Diagram

The simplified process flow diagram for the purpose of MATLAB studies can be referred in *Figure 1.1* below. Basically, this design comes from the conceptual design of Douglas J.M [9] and the operating condition of Ahmad et al. [16]. *Figure 1.2* on the next page section is the overall process flow diagram of the bio-oil steam reforming. By designing the process flow diagram, one can focus and understand the concept of steam reforming process flow. The feed for this process is bio-oil and water. The details about the functions of each operating units can be referred in the *Appendix 1* section.

According to the *Figure 1.2*, the three dotted circles are the main operating units that will be involved for the MATLAB feasibility studies. The first unit is the steam reformer, in which steam-reforming process of bio oil will take place. The second unit is the water gas shift reactor, in which water gas shift reaction will occur. Finally, the PSA column, where the purification of hydrogen will take place.

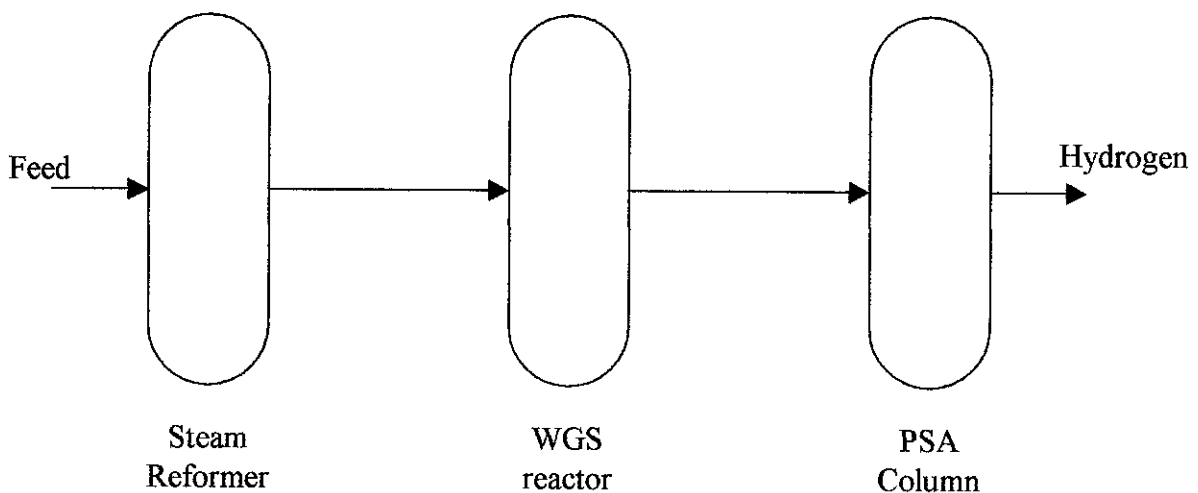


Figure 1.1: Simplified Process Flow Diagram

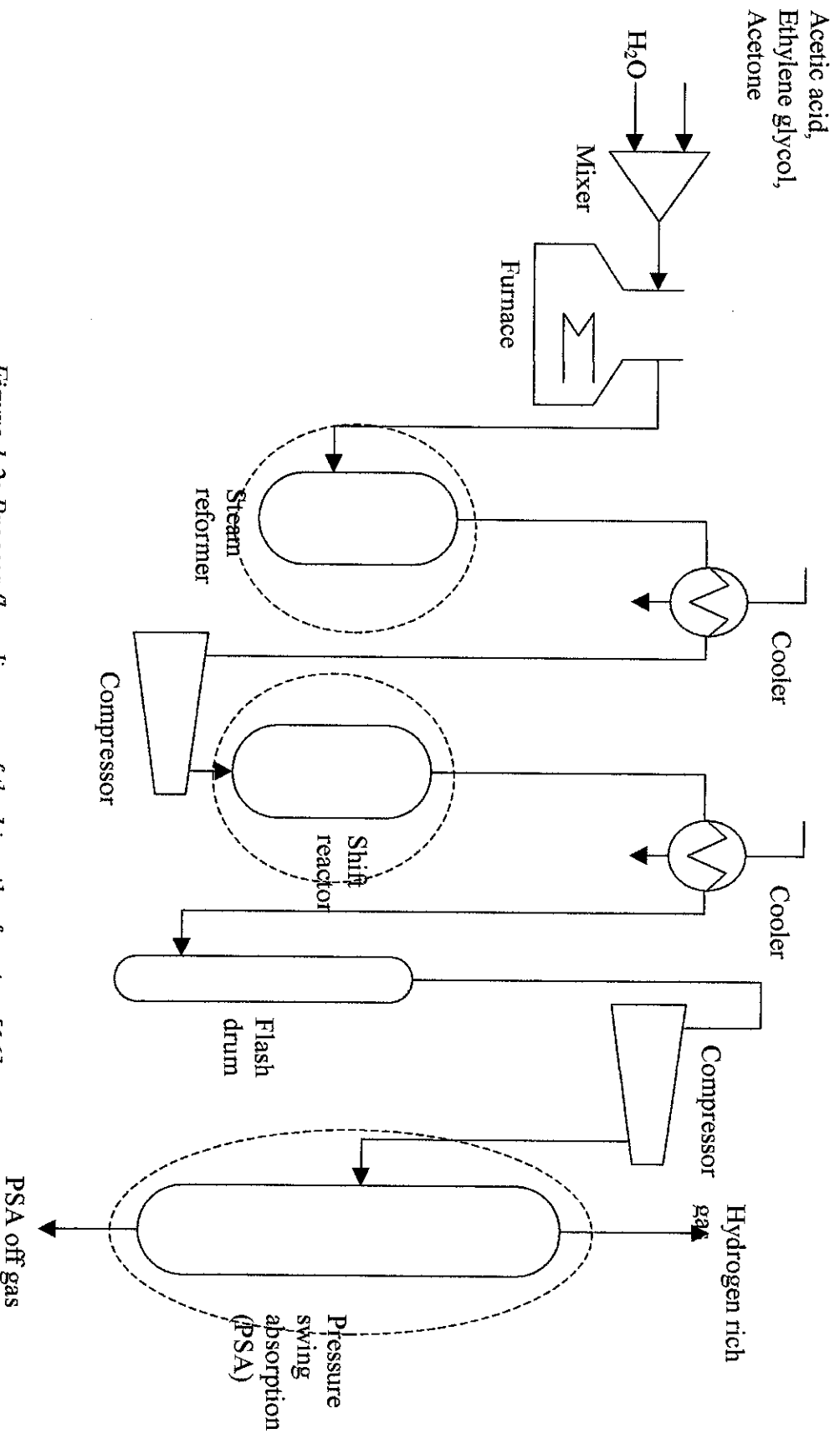


Figure 1.2: Process flow diagram of the bio-oil reforming [16]

1.5 Problem Statement

There exists a wide range of modeling approaches to represent hydrogen production from bio oil via steam reforming. It is known that, modeling approach, even it is less expensive and more extendable compared to experimental procedures, has its own limitation. Different model has its different strength and limitation, in which will indicate it is an accessible model or otherwise. This project will aim to review and to put up models that can represent each process step in hydrogen production from bio oil in a simplest way.

Due to some difficulties of finding the necessary journals regarding the kinetic modeling of the bio oil, the bio oil will be represented by crude ethanol. It is assumed that the use of crude ethanol kinetic modeling somehow replicate the kinetic modeling of bio oil, as the molecular formula of crude ethanol is $C_{2.12}H_{6.12}O_{1.23}$, which is somewhat similar to the basic molecular formula of bio oil, $C_{1.8}H_{4.12}O_{1.54}$ obtain from Rioch CE et al. [2]. The crude ethanol steam reforming general equation can be represented as:



Crude Ethanol Components	Volume %	Mole % on a water free basis
Ethanol	12.0	88.42
Lactic acid	1.0	5.71
Glycerol	1.0	5.87
Maltose	0.001	0.001
Water	86.0	Not applicable

Table 1.1: Crude Ethanol Composition [10]

However, for the purpose of simplicity, the stoichiometry of ethanol is used to develop the kinetics, as it is well known.

1.6 Objective

1. To screen suitable models to represent hydrogen production from bio-oil via steam reforming. The bio oil has been represented by ethanol, in which the kinetic modeling will replicate the kinetic modeling of bio oil.
 - a. By referring to the work of Akande etc [10], the modeling approach for steam reforming for ethanol can be done.
 - b. The work is found suitable, as the bio oil has been represented by ethanol.
2. The models of each process step in hydrogen production are compiled by MATLAB.
 - a. The process steps from steam reforming to water gas shift reaction, to PSA purification of hydrogen are gathered into one system so that the molar balance can be determined.
3. To develop the modeling ways and then used to simulate the sequence of processes in hydrogen production from bio-oil in MATLAB.
 - a. To determine the significance of this work and then to compare the results of this work with other previous works.
 - b. To find out if this work has an advantage compared to the other works.

CHAPTER 2: LITERATURE REVIEW

This chapter summarizes the suitable journals or works in order to be used for references of this project. The journals contain the appropriate information such as theories, equations and also result that will be sufficient to carry out the project. Below are the summaries of all the suitable journals that are related to the project that managed to be found. Since there will be three main processes involved in this project, the necessary journals are crucial so that the system will work.

2.1 Steam Reforming

Journal/ Paper	Author	Description
Kinetic Modeling of Hydrogen production by the catalytic reforming of crude ethanol over a co-precipitated Ni-Al ₂ O ₃ catalyst in a packed bed tubular reactor. [10]	<ul style="list-style-type: none"> ▪ Abayomi Akande ▪ Ahmed Aboudheir ▪ Raphael Idem ▪ Ajay Dalai. 	<ul style="list-style-type: none"> ▪ The kinetic modeling of H₂ production has been performed over 15% Ni-Al₂O₃ catalyst. ▪ The kinetic experiment was done at atmospheric pressure in packed bed tubular reactor at temperature 593-793 K. ▪ Eley Rideal assumptions where the surface reaction involved an absorbed species and a free gaseous were used to develop the reaction mechanism and four models were proposed. ▪ The model of dissociation of adsorbed crude ethanol as rate determining step was develop. ▪ The model was $r_A = (2.08 \times 10^{-8} e^{-4430/RT})(N_A) / [1 + 3.83 \times 10^7 N_A]^2$ ▪ Absolute deviation between experimental rates and predicted rates was 6% for this model.
Ethanol steam reforming in a dense Co-Ag membrane reactor: A modeling work. Comparison with the traditional steam. [22]	<ul style="list-style-type: none"> ▪ F. Gallucci ▪ M. De Falco ▪ S. Tosti ▪ L. Marrelli ▪ A. Basile 	<ul style="list-style-type: none"> ▪ Mathematical model has been formulated for a traditional reactor packed with a Co-based catalyst and then applied to a membrane reactor (MR). ▪ With MR reactor, high conversion of ethanol and high hydrogen selectivities.

These two works are compared to determine which has the ideal modeling approaches. After a few studies, the work of Akande et al. [10] seems to be the right journal to be referred to as it has the necessary information in order to develop a model for steam reforming of ethanol.

Basically, the work of Akande et al. [10] is focused more on the hydrogen production by the catalytic reforming of crude ethanol over a co-precipitated $Ni-Al_2O_3$ catalyst in a packed bed tubular reactor. This method is a tradition to steam reforming process compared to the work of Gallucci et al. [22], which it uses the more conventional method, the membrane reactor.

In theory, the performance of the membrane reactor was compared with the traditional reactor in the journal of Gallucci et al. [22]. It indicates that using the membrane reactor with the respect to the traditional reactor can increase the ethanol conversion. Moreover, a CO -free hydrogen stream can be directly produced in the membrane reactor and it can be directly fed to a proton exchange membrane fuel cell system.

But, the journal of Gallucci et al. [22] does not have complete information on how to develop the modeling for steam reforming. Thus, it is decided that the work of Gallucci et al. [22] will be put aside although the used of membrane reactor for steam reforming is very practical and feasible in theory.

2.2 Water Gas Shift Reaction.

Journal/ Paper	Author	Description
Water gas shift reaction kinetics and reactor modeling for fuel cell grade hydrogen [11]	<ul style="list-style-type: none"> ▪ Yongtaek Choi ▪ Harvey G. Stenger 	<ul style="list-style-type: none"> ▪ The reaction was studied to evaluate existing reaction mechanisms. ▪ To test various rate expressions and to simulate the performance in a methanol fuel processor for fuel cell applications. ▪ The reaction was done in a micro reactor-testing unit using a commercial Sud-Chemie $Cu/ZnO/Al_2O_3$ catalyst between 120-250 °C with a range of feed rates and compositions. ▪ Using non-linear least squares optimization, the parameters in five rate expressions were fit to the experimental data. ▪ Numerical integration of a one-dimensional PFR model was used for this parameter fitting. ▪ An empirical rate expression, $r_{CO} = kP_{CO}P_{H_2O} (1 - \beta)$ with activation energy of 47.4 kJ/mol was obtained from the experiment. ▪ Reactor performance was simulated to determine catalyst loadings required to achieve specific CO conversions as a function of temperature and water feed rate
Modeling of CO ₂ -selective water gas shift membrane reactor for fuel cell [18]	<ul style="list-style-type: none"> ▪ Jin Huang ▪ Louei El-Azzami ▪ W.S. Winston Ho 	<ul style="list-style-type: none"> ▪ WGS reaction is critical to hydrogen purification for fuel cells. ▪ WGS reaction in the traditional fixed bed reactor is not efficient. ▪ Using a CO₂-selective membrane reactor shifts the reaction towards the product side, ▪ Which enhances the conversion of CO and increases the purity of the H₂ product at a high pressure. ▪ Using a one-dimensional non-isothermal model simulated the simultaneous reaction and transport process in the countercurrent WGS membrane reactor. ▪ The effect of several system parameters including CO₂/H₂ selectivity, CO₂ permeability, and sweep-to-feed molar flow rate ratio were investigated.

The work of Choi et al. [11] and Huang et al. [18] are compared so that the modeling approach for water gas shift reaction can be developed. It seems that theoretically, the work of Huang et al. [18] is much better in enhancing the conversion of CO and increases the purity of the H_2 production at high pressure compared to the traditional shift reactor, which is fixed bed reactor. The journal of Huang et al. [18] also has done some investigation on the effect of several system parameters including CO/H_2 selectivity, CO_2 permeability, and sweep to feed molar flow rate ratio.

But, the work of Huang et al. [18] does not have the information regarding the rate of reaction for CO , whereas for the work of Choi et al. [11], it has the equation for rate of reaction for CO , although the use of fixed bed reactor is not very practical in enhancing the conversion of CO and increasing the purity of H_2 production. Even though it is not very efficient, it has the proper modeling equations that is called empirical fitting rate expression derived from the numerical fitting, which will be accurate and much more simple.

2.3 Hydrogen Purification

Journal/ Paper	Author	Description
A parametric study of layered bed PSA for hydrogen purification [12]	<ul style="list-style-type: none"> ▪ Ana M. Ribeiro ▪ Carlos A. Grande ▪ Filipe V.S. Lopes ▪ José M. Loureiro ▪ Alírio E. Rodrigues 	<ul style="list-style-type: none"> ▪ This work is focused on the separation of hydrogen from a five-component mixture ($H_2/CO_2/CH_4/CO/N_2$) by pressure swing absorption. ▪ The mathematical model of this paper is applied in the study of the behavior of single column and four column PSA processes with layered activated carbon and with an eight-step cycle. ▪ 99.994% purity of H_2 is attained at the end of the feed step for a process hydrogen recovery of 51.84% and a productivity of $59.6 \text{ mol}_{H_2} / \text{kg}_{\text{ads}} / \text{day}$. ▪ Multicolumn simulation predicts a H_2 recovery and purity, 52.11% and 99.995% respectively. ▪ Activated carbon layer improves both the purity and recovery of the process.

Basically, for the purification of hydrogen, only journal of Ribeiro et al. [12] is suitable to develop a model of this process. This work is focused on the separation of hydrogen from a five-components mixture, which is H_2 , CO_2 , CH_4 , CO , and N_2 by a separation technique namely as pressure swing absorption. This work tells that a complete model is able to describe the dynamic behavior of the pressure swing adsorption system. This work also shows that activated carbon layer will improve both the purity and recovery of the hydrogen purification process.

The mass balance equation for gas phase of a fixed bed system is applied in order to determine the amount of hydrogen produced after PSA column. By referring to the table of boundary condition from Ribeiro et al. [12], it is assumed that co-current pressurization with feed will determine the amount of hydrogen production for the purification system.

CHAPTER 3: METHODOLOGY

3.1 Overview of Overall Project Methodology

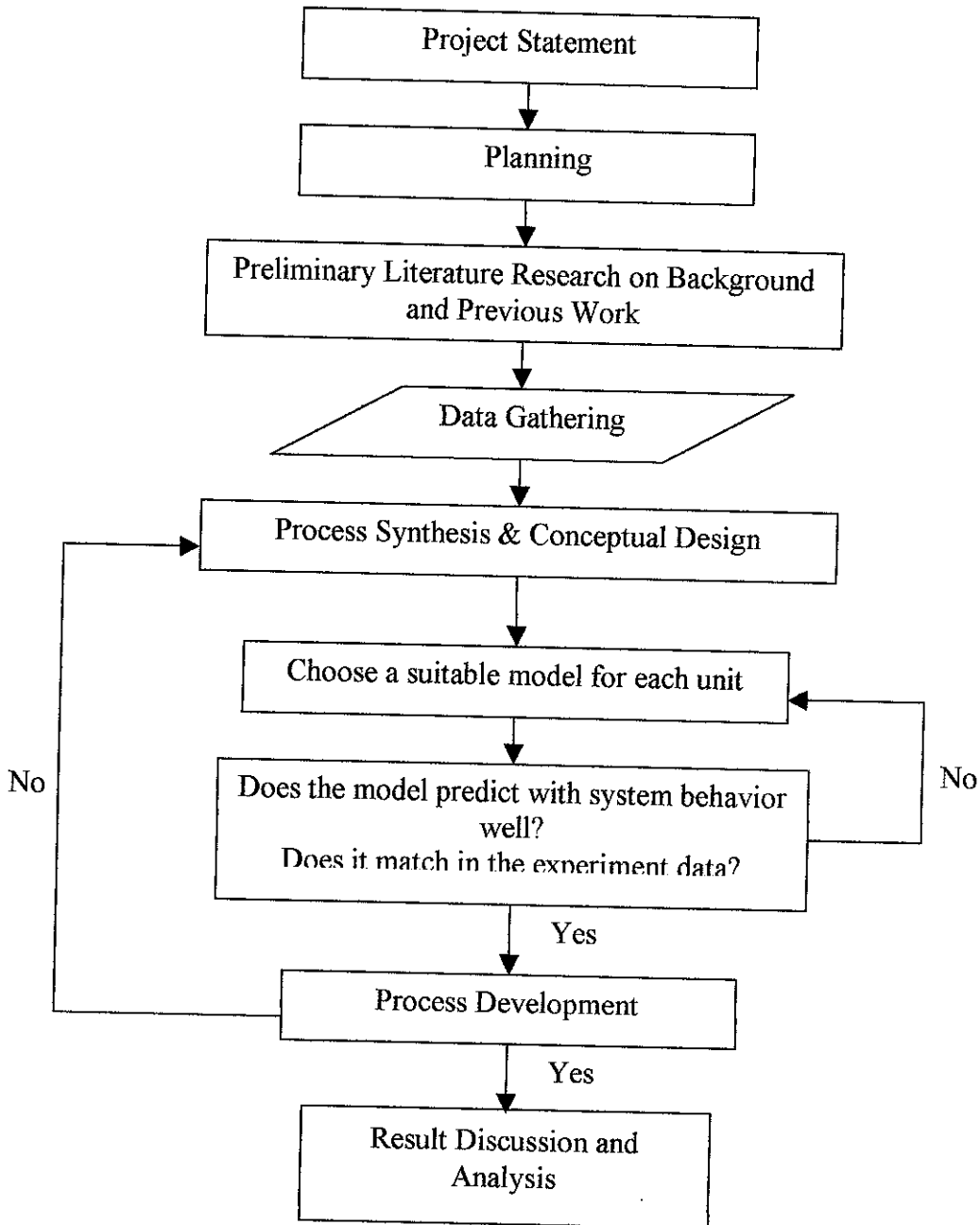


Figure 3.1: Block Diagram of Project Methodology

Project Statement

- The FYP begins when the project that shall be chosen will get the supervisor's approval.

Planning

- Good planning on the project development will help on the direction of the project to avoid any lost in project track.

Preliminary Literature on Background and Previous Work Research

- Necessary journals and work will be sufficient in order to understand the basic concept of the project.

Data Gathering

- After obtaining the right journals and works, it is better to gather all of the data so that any problems regarding the project can easily be referred back to the information gathered.

Process Synthesis & Conceptual Design

- Building the design of the operating units to comprehend the concept of the process involved.

Choose a suitable model for each unit

- A suitable model is important to a unit so that the model can be checked whether it converges or otherwise.

Does the model predict with system behavior well? Does it match in the experiment data?

- A proper investigation is needed so that any inaccuracy will be quickly discarded so that the model will match the experiment data.

Process Development

- If no problem occurs, then the project will be commenced as usual.

Result Discussion and Analysis

- Finally, the project will be summarized and analysis will be made.

3.2 Project Gant Chart

For this work, it was initially divide into two continuing sessions (FYP 1 and FYP 2), which will be carried out for two semesters. For the FYP1 the project work is more on emphasizing on the literature modeling research and development. Whereas for the FYP2, the project work will be more on writing the modeling programming language by using MATLAB. Basically, the details of the project work for FYP 1 and FYP 2 are illustrated in *Appendix 2* and *Appendix 3*.

3.3 Process Development

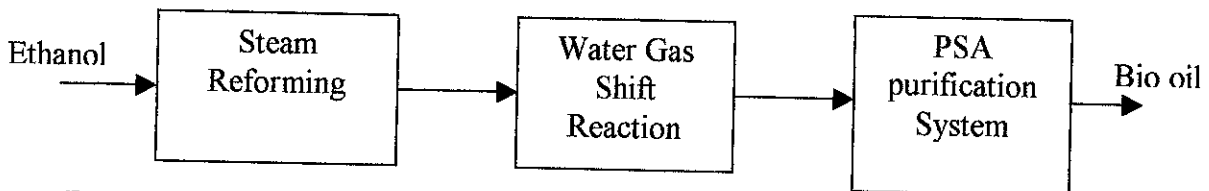


Figure 3.2: Block Diagram Each Step Process in Hydrogen Production from Ethanol

Steam Reforming

- The journal of Akande et al. [10] is used to determine the rate of reaction of ethanol and the work of Koumpouras et al. [21] is used to determine the component balance for all components in the reactor reformer.
- Model assumptions
 - Steady state and non isothermal (adiabatic) operation
 - Perfect gas behavior
 - Adsorption kinetics described by linear driving force model (LDF) and Langmuir isotherm for CO_2 adsorption equilibrium.
 - The general kinetics from Akande et al. [10] is used to determine the accumulation of hydrogen production.

- CO_2 is considered as the only adsorbate and CO_2 adsorption is assumed to take place on the flowing adsorbent particle.
- Ideal plug flow
- Gas and adsorbent particle velocities are assumed constant and equal.

Water Gas Shift Reaction

- The work of Choi et al. [11] and Huang et al. [18] are used to obtain the modeling approach for the rate of reaction of CO and also the component balance in the shift reactor.
- Model assumptions
 - CO_2 and H_2 are the only two gasses permeating through the membrane.
 - There is no temperature variation in the radial direction inside a hollow fiber due to its small dimension/
 - Membrane permeability is fixed and does not change with temperature variation.
 - The module is adiabatic and operates at steady state.
 - There is no axial mixing.
 - The pressure drops on both lumen and shell sides are negligible.

PSA Purification System

- The work of Ribeiro et al. [12] is used to obtain the mathematical model of component balance equation in a fixed bed adsorption system.
- Model assumptions
 - Ideal gas behavior throughout the column, within the operating conditions under study, the gases follow nearly the ideal gas law.
 - No mass, heat or velocity gradients in the radial direction.
 - External mass and heat transfer resistances, both expressed with the linear driving force model (LDF).
 - Constant porosity along the bed.
 - No temperature gradients inside each particle as the heat transfer in the solid particles are much higher than in the gas phase.

CHAPTER 4: RESULTS AND DISCUSSION

4.1 Steam Reforming of Crude Ethanol

4.1.1 The calculation of rate of reaction

For the Steam Reforming, the work by Akande et al. [10] is used to obtain the modeling equations. In this study, crude ethanol conversion (X) was evaluated in terms of ethanol plus other organics on a water free basis as shown in the following equation:

$$\text{Crude Ethanol Conversion (X)} = \frac{\text{gmol (organics) in} - \text{gmol (organics) out}}{\text{gmol (organics) in}}$$

Where organics = ethanol + lactic acid + glycerol + maltose.

Based on the experimental data of Akande et al. [10], the results for the variation of crude ethanol conversion X with ratio of weight of catalyst to crude ethanol flow rate ratio (W/F_{A0}) at reaction temperatures of 593, 693, and 793 K are presented in *Figure 4.1* [10].

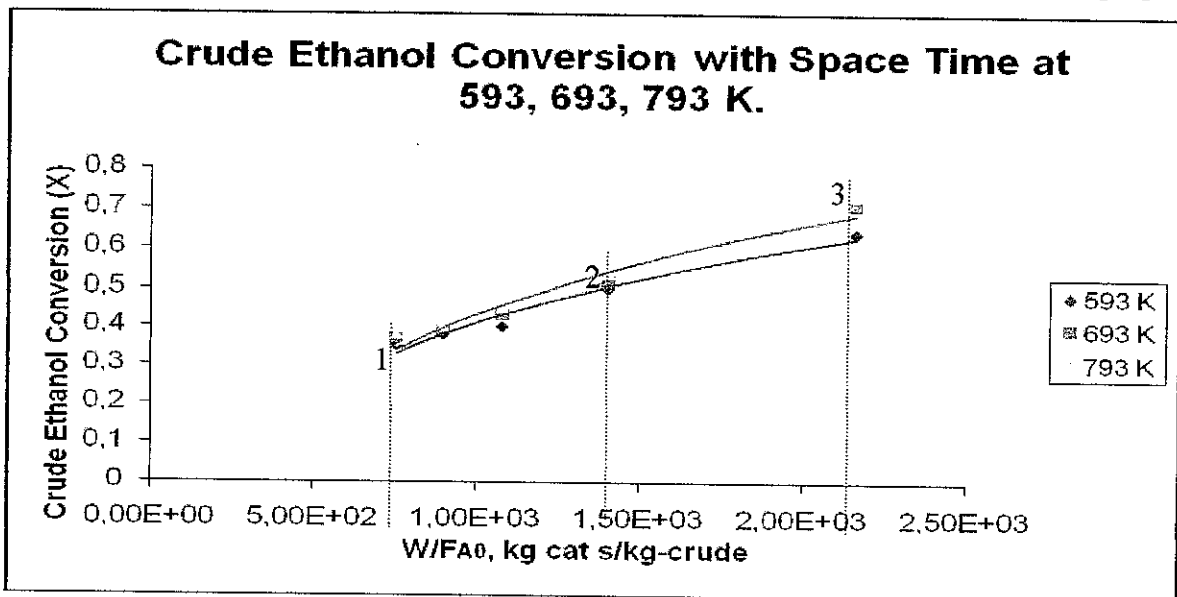


Figure 4.1: Variation of crude ethanol conversion with space time [10]

According to Akande et al. [10], a micro reactor was used to gather the experimental data and the design equation for the plug flow reactor was therefore applicable for data analysis. This was used in the differential form.

$$\frac{dX}{d(W / F_{A0})} = r_A$$

To determine the predicted rate of equation, r_A various slopes were taken at each of the three temperatures in order to differentiate with the measured rate of equation, r_A of all three models. The slopes of each of the points were calculated manually. Based on *Figure 4.1*, only three points **(1)** 7.56×10^2 , **(2)** 1.4×10^3 , **(3)** 2.16×10^3 were taken at each temperature because in this project, the measured r_A are calculated with only 3 trials.

For the temperature of 593 K;

$$\begin{aligned} r_A &= \frac{0.65 - 0.585}{2300(46.07) - 1880(46.07)} \\ &= 3.36 \times 10^{-6} \end{aligned}$$

$$\begin{aligned} r_A &= \frac{0.54 - 0.45}{1620(46.07) - 1140(46.07)} \\ &= 4.096 \times 10^{-6} \end{aligned}$$

$$\begin{aligned} r_A &= \frac{0.39 - 0.315}{980(46.07) - 700(46.07)} \\ &= 5.814 \times 10^{-6} \end{aligned}$$

Thus, by doing the same method of finding the value of the slope (predicted r_A) to both temperature, value of each slopes are represented in *Table 4.1*

Points Temperatures	1	2	3
593 K	5.814×10^{-6}	4.096×10^{-6}	3.36×10^{-6}
693 K	7.96×10^{-6}	4.65×10^{-6}	2.71×10^{-6}
793 K	9.41×10^{-6}	5.42×10^{-6}	4.34×10^{-6}

Table 4.1: Value of slopes (predicted r_A) at temperature 593, 693, 793 K

Based on Akande et al. [10], in order to calculate the value of r_A , four models have to be chosen that will be the most realistic to the catalytic reforming of crude ethanol over Ni-Al₂O₃ catalyst. In the journal, it states that there are four cases as possible rate controlling mechanisms for the catalytic reforming of crude ethanol. Table 4.2 and Table 4.3 are obtained from the work of Akande et al. [10].

Table 4.2: Table of kinetic models [10]

RDS	Models based on species molar flow
Adsorption of crude ethanol	$r_A = \frac{k_{oc}^{-E/RT} \left[N_A - \frac{N_C^2 N_D^6}{K_P N_B^3} \right]}{\left[1 + \frac{K_F N_C N_D^3}{N_B} + \frac{K_G N_C N_D^3}{N_B^2} + \frac{K_E N_C^2 N_D^6}{N_B^3} \right]}$
The dissociation of adsorbed crude ethanol	$r_A = \frac{k_{oc}^{-E/RT} \left(N_A - \frac{N_C^2 N_D^6}{K_P N_B^3} \right)}{\left[1 + K_A N_A + \frac{K_F N_C N_D^3}{N_B} + \frac{K_G N_C N_D^3}{N_B^2} \right]^2}$
Surface reaction between adsorbed oxygenated hydrocarbon and steam	$r_A = \frac{k_{oc}^{-E/RT} \left(\frac{N_A N_B^3}{N_C N_D^3} - \frac{N_C N_D^3}{K_P} \right)}{\left(1 + K_A N_A + \frac{K_Q N_A N_B^2}{N_C N_D^3} + \frac{K_G N_C N_D^3}{N_B^2} \right)}$
Surface reaction between adsorbed s hydrocarbon fraction species and steam	$r_A = \frac{k_{oc}^{-E/RT} \left(\frac{N_A N_B^3}{N_C N_D^3} - \frac{N_C N_D^3}{K_P} \right)}{\left(1 + K_A N_A + \frac{K_F N_C N_D^3}{N_B} + \frac{K_H N_A N_B}{N_C N_D^3} \right)}$

Table 4.3: Nomenclature for catalytic reforming of crude ethanol [10]

Nomenclature			
r_A	rate of crude-ethanol conversion, kmol crude/kg cat s	N_i	molar flow rate of species kmol/s
E	activation energy, kJ/kmol	RDS	rate-determining step
k_0	collision frequency or pre-exponential constant, (kg cat s) ⁻¹	W	weight of catalyst, kg
K_i	equilibrium constant of reaction step i	X	crude-ethanol conversion mol% or fractional conversion
K_p	overall equilibrium constant	AAD%	average absolute deviation, %
R	universal gas constant, kJ/kmol K	W/F_{A0}	space time, kg cat s/kg crude

The Power Law model is used to fit the experimental data.

$$r_A = k_0 e^{-E/RT} (N_A)^n$$

Let $C_2H_6O = A$;
 $H_2O = B$;
 $CO_2 = C$;
 $H_2 = D$;

It is decided to choose only three models of rate of reaction, r_A that will be compared with the predicted rate of reaction, r_A . The models are adsorption of crude ethanol (*model 1*), the dissociation of adsorbed crude ethanol (*model 2*), and also *power law model*. Then, the r_A is calculated using the models in MATLAB. For the calculation of model 1, the equations and variables are written in *.m format and then it is saved by the name of **steam_reforming_model1.m**. The same method is applied to the other two models, which are model 2, and power law model. The names of the files of those two models are **steam_reforming_model2.m** and **power_law_model.m**. The MATLAB programs can be referred in *Appendix 4*, *Appendix 5* and *Appendix 6* for more details.

Table 4.4 is the kinetic experimental data, which shows the molar flow for each species for catalytic reforming of crude ethanol [10]. With these data, the calculation of r_A can be

done. *Table 4.5* is the fitted values of kinetic constant of crude ethanol and *Table 4.6* is the summary of all the measured r_A for the three models along with the predicted r_A .

Table 4.4: Kinetic experimental data for catalytic reforming of crude ethanol [10]

T (K)	N_A (kmole/s)	N_B (kmole/s)	N_C (kmole/s)	N_D (kmole/s)	K_P
593	5.70596E-09	1.57331E-07	8.40614E-09	2.40685E-08	2.45431E+11
593	8.43861E-09	2.0793E-07	8.81142E-09	2.52289E-08	2.45431E+11
593	1.64558E-08	3.51408E-07	9.27356E-09	2.65521E-08	2.45431E+11
693	5.02195E-09	1.57821E-07	1.0229E-08	2.92878E-08	3.36674E+15
693	9.80704E-09	2.41648E-07	1.02403E-08	2.93201E-08	3.36674E+15
693	1.73306E-08	3.66116E-07	9.18524E-09	2.62993E-08	3.36674E+15
793	5.11495E-09	1.60744E-07	1.04184E-08	2.98302E-08	4.45742E+18
793	8.52993E-09	2.21894E-07	1.06204E-08	3.04085E-08	4.45742E+18
793	1.62475E-08	3.50781E-07	9.71516E-09	2.78165E-08	4.45742E+18

Table 4.5: Fitted values of kinetic constants of crude ethanol reforming to hydrogen based on model 1, model 2 and power law [10]

Parameter	Model # 1.	Model # 2.	Power law
K_O	8.91×10^2	2.08×10^3	3.12×10^{-2}
E	4.03×10^3	4.43×10^3	4.41×10^3
K_A	—	3.83×10^7	—
K_E	0.0	—	—
K_F	0.0	0.0	—
K_G	0.0	0.0	—
K_H	—	—	—
K_Q	—	—	—
n	—	—	0.43
ADD	20.6%	6.0%	4.5%

Temp, K	Model 1	Model 2	Power Law Model	Predicted r_A , kg mol/kg cat s
	Measured r_A , kg mol/kg cat s	Measured r_A , kg mol/kg cat s	Measured r_A , kg mol/kg cat s	
593	2.25E-06	3.25E-06	3.64E-06	3.36E-06
593	3.32E-06	4.08E-06	4.31E-06	4.07E-06
593	6.47E-06	5.24E-06	5.74E-06	5.81E-06
693	2.22E-06	3.41E-06	3.92E-06	2.17E-06
693	4.34E-06	5.00E-06	5.23E-06	4.65E-06
693	7.67E-06	6.04E-06	6.67E-06	7.96E-06
793	2.26E-06	3.45E-06	3.95E-06	4.34E-06
793	3.78E-06	4.67E-06	4.92E-06	5.43E-06
793	7.19E-06	5.95E-06	6.49E-06	9.41E-06

Table 4.6: The values of the measured r_A for the three models along with the predicted r_A .

Figure 4.3 represents the parity chart of comparison between the measured rates and predicted rates using the three rate models. The use of parity chart will be beneficial so that the comparison can be made significantly by just observing the pattern of the chart. This chart resembles the chart used in Akande etc [10] in order to differentiate and to compare the measured and predicted rates of rate models.

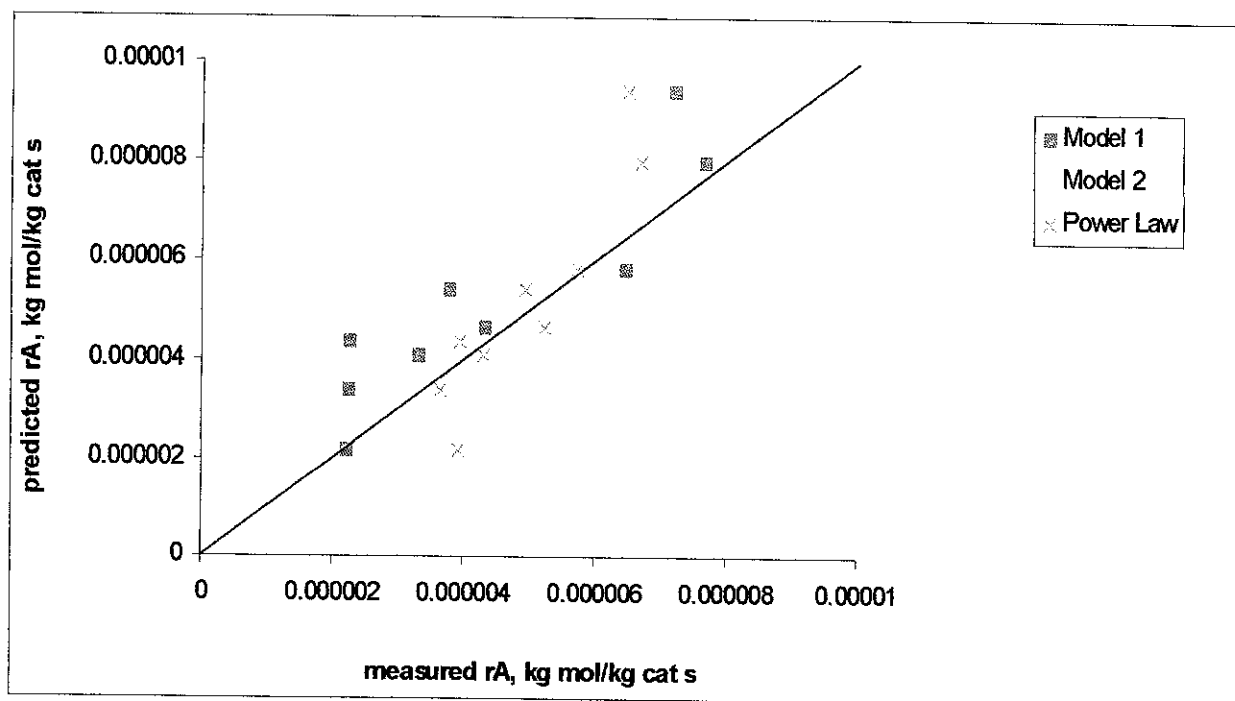


Figure 4.2: A comparison of measured and predicted rates of reforming crude ethanol within the temperature range of 593-793 K [10]

A closer look at the chart, one can assume that model 1 did not yield a satisfaction result. This is because the average relative error for model 1 is high, which is 29.1% (>25%). Whereas for model 2 and power law, the average relative error are 21.1% and 17.2% respectively (<25%).

The calculation of average relative error of all the three models can be referred in *Table 4.7, 4.8, 4.9.*

Table 4.7: Model 1 average relative error.

Temp, K	Model 1 Measured r_A , kg mol/kg cat s	Predicted r_A , kg mol/kg cat s	Model 1 Relative error
593	2.25E-06	3.36E-06	4.97E-01
593	3.32E-06	4.07E-06	2.26E-01
593	6.47E-06	5.81E-06	1.02E-01
693	2.22E-06	2.17E-06	2.39E-02
693	4.34E-06	4.65E-06	7.11E-02
693	7.67E-06	7.96E-06	3.75E-02
793	2.26E-06	4.34E-06	9.17E-01
793	3.78E-06	5.43E-06	4.37E-01
793	7.19E-06	9.41E-06	3.08E-01
		Average	2.91E-01

Table 4.8: Model 2 average relative error.

Temp, K	Model 2 Measured r_A , kg mol/kg cat s	Predicted r_A , kg mol/kg cat s	Model 2 Relative error
593	3.25E-06	3.36E-06	3.26E-02
593	4.08E-06	4.07E-06	2.89E-03
593	5.24E-06	5.81E-06	1.08E-01
693	3.41E-06	2.17E-06	3.64E-01
693	5.00E-06	4.65E-06	6.94E-02
693	6.04E-06	7.96E-06	3.18E-01
793	3.45E-06	4.34E-06	2.59E-01
793	4.67E-06	5.43E-06	1.62E-01
793	5.95E-06	9.41E-06	5.81E-01
		Average	2.11E-01

Table 4.9: Power Model average relative error.

Temp, K	Power Law Model		Power Law Model Relative error
	Measured r_A , kg mol/kg cat s	Predicted r_A , kg mol/kg cat s	
593	3.64E-06	3.36E-06	7.64E-02
593	4.31E-06	4.07E-06	5.46E-02
593	5.74E-06	5.81E-06	1.27E-02
693	3.92E-06	2.17E-06	4.47E-01
693	5.23E-06	4.65E-06	1.10E-01
693	6.67E-06	7.96E-06	1.93E-01
793	3.95E-06	4.34E-06	9.90E-02
793	4.92E-06	5.43E-06	1.03E-01
793	6.49E-06	9.41E-06	4.50E-01
		Average	1.72E-01

With these results, it is concluded that the 2nd model of dissociation of adsorbed crude ethanol, is on the active site of the rate determining steps as the average relative error seems to be much lesser comparing to the 1st model, which is 21.1%. Besides that, the power model is also on the active site of the rate determining steps, as the average relative error is less than 25%, which is 17.2%.

With these, the value of measured r_A of Power Law Model for each temperature 593 K, 693 K and 796 K are gathered in order to find the average. Table 4.10 shows the calculated average for each temperature for Power Law Model.

Table 4.10: Calculated Average for each Temperature for Power Law Model

Temperatures \ Trials	Trials			Average
	1	2	3	
593 K	3.64E-06	4.31E-06	5.74E-06	4.47E-06
693 K	3.92E-06	5.23E-06	6.67E-06	5.27E-06
793 K	3.95E-06	4.92E-06	6.49E-06	5.12E-06

Then, each average value of r_A for each temperature will be manually estimated on *Figure 4.1* by spotting the average value within the appropriate points. Let say, for average r_A of 593 K, which is 4.47E-06 kg mol/kg cat s, the value is somehow located between point 1 and point 2. Thus, the conversion, X for r_A of 4.47E-06 kg mol/kg cat s is estimated 0.45. The same method is applied to the rest of r_A so that the conversion, X for each r_A can be determined. *Table 4.11* shows the conversion, X for each average r_A .

Table 4.11: Conversion, X of Calculated Average for each Temperature for Power Law Model

Temperature, K	Average r_A , kg mol/kg cat s	Conversion, X
593	4.47E-06	0.45
693	5.27E-06	0.49
793	5.12E-06	0.6

With the value of conversion, X for each r_A obtained, the amount of products produced after the steam reforming reactor can be determined by using the equation below obtained from the work of Akande etc [10]:

$$\text{Conversion, } X = \frac{\text{kg / hr(in)} - \text{kg / hr(out)}}{\text{kg / hr(in)}}$$

According to [16], the amount of feed is 1200 kg/hr. The value of conversion, X is 0.6 because it is assumed that 793 K is the final temperature that will exit the reactor. Thus, by doing the back calculation to get the amount of product after the steam reforming reactor:

$$0.6 = \frac{1200 \text{ kg/hr} - \text{kg/hr (out)}}{1200 \text{ kg/hr}}$$

$$720 = 1200 \text{ kg/hr} - \text{kg/hr (out)}$$

$$\text{Out} = 480 \text{ kg/hr (organics)}$$

Where organics = ethanol + lactic acid + glycerol + maltose

4.1.2 The calculation of Component Balance

Based on the work of Koumpouras et al. [21], the component balance of gas phase can be represented as:

$$-u_g \frac{dn_{i,g}}{dz} - \varepsilon \varphi \mathcal{G}_{ads} r_{ads} - k_m \frac{2}{R_c} \varepsilon (n_{i,g}) = 0$$

Where

- u_g = superficial velocity
- = 0.46 ms^{-1}
- $n_{i,g}$ = molar flowrate i of outlet gas mol s^{-1}
- $n_{i,f}$ = molar flowrate i of feed gas mol s^{-1}
- k_m = mass transfer coefficient
- = 0.15 ms^{-1}
- R_c = monolith channel radius, $\text{m} = 1 \times 10^{-3} \text{ m}$
- ε = 0.5 (dimensionless)
- φ = 0.1 (dimensionless)
- \mathcal{G}_{ads} = 1563 kg m^{-3}
- r_{ads} = r_A (obtained from the measured of rate of reaction of Power Law Model)
- = $3.64 \times 10^{-6} \text{ kg}$

B.C. 1 at $z=0$, $n_{i,g}=n_{i,f}$

$$-(0.46)\frac{dn_{i,g}}{dz} - (0.5)(0.1)(1563)(3.64 \times 10^{-6}) - 0.15\frac{2}{(0.001)}(0.5)(n_{i,f}) = 0$$

Simplified

$$\frac{dn_{i,g}}{dz} = -326.1(n_{i,f}) - 6.174 \times 10^{-4}$$

Integrate both sides

$$\int \frac{dn_{i,g}}{dz} = \int -326.1(n_{i,f}) - \int 6.174 \times 10^{-4}$$

$$n_{i,g} = -326.1(n_{i,f})z - 6.174 \times 10^{-4}z + c$$

B.C. 2 at $z=L=0.15$,

Based on the Huang et al. [18], the $n_{i,g}$ for each components are:

$$n_{CO,g} = 6.35 \times 10^{-3} \text{ mol/s}$$

$$n_{H_2O,g} = 0.11557 \text{ mol/s}$$

$$n_{H_2,g} = 0.4134 \text{ mol/s}$$

$$n_{CO_2,g} = 0.09843 \text{ mol/s}$$

$$n_{CH_4,g} = 1.27 \times 10^{-3} \text{ mol/s}$$

For CO

$$6.35 \times 10^{-3} = -326.1(n_{CO,f})(L) - 6.174 \times 10^{-4}(L) + c$$

$$c = 6.35 \times 10^{-3} + 326.1(n_{CO,f})(L) + 6.174 \times 10^{-4}(L)$$

For H_2O

$$c = 0.11557 + 326.1(n_{H_2O,f})(L) + 6.174 \times 10^{-4}(L)$$

For H_2

$$c = 0.11557 + 326.1(n_{H_2,f})(L) + 6.174 \times 10^{-4}(L)$$

For CO_2

$$c = 0.09843 + 326.1(n_{CO_2,f})(L) + 6.174 \times 10^{-4}(L)$$

For CH_4

$$c = 0.11557 + 326.1(n_{H_2,f})(L) + 6.174 \times 10^{-4}(L)$$

Thus, the amount of feed of the reformer reactor for each component is:

For CO

$$6.35 \times 10^{-3} = -326.1(n_{CO,f})(0.15) - 6.174 \times 10^{-4}(0.15) + 6.35 \times 10^{-3} + 326.1(n_{CO,f})(0.15) + 6.174 \times 10^{-4}(0.15)$$

Solve

$$n_{CO,f} = 0$$

The feed that entered the steam reformer reactor contains only ethanol C_2H_6O . Thus, all components such as CO , H_2O , H_2 , CO_2 , and CH_4 are not contained in the feed stream.

So,

$$\text{For } H_2O, \quad n_{H_2O,f} = 0$$

$$\text{For } H_2, \quad n_{H_2,f} = 0$$

$$\text{For } CO_2, \quad n_{CO_2,f} = 0$$

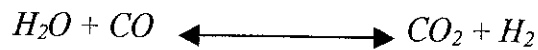
$$\text{For } CH_4, \quad n_{CH_4,f} = 0$$

$$\text{For } C_2H_6O, \quad n_{C_2H_6O,f} = n_{b,f} = 0.635 \text{ mol s}^{-1} \text{ (ethanol feed that enters reformer based on Huang et al. [18])}$$

4.2 Water Gas Shift Reaction

4.2.1 The calculation of rate of reaction

For the water gas shift reaction, the work of Choi et al. [11] is used to obtain the modeling equations. In this study, a number of rate expressions have been reported and tested to evaluate the water gas shift reaction rate for various catalyst:



According to the work of Choi et al.[11], they focused on the condition of temperature and pressure as they used a small reactor in an ethanol reformer for a PEM fuel cell. Basically, in the real industry, WGS reactor operates at a very high temperature and pressure. With the catalyst of Sud-Chemie $Cu/ZnO/Al_2O_3$, which is a commercial catalyst, the reaction kinetics and mechanism for the water gas shift reaction have been studied by them.

In this work, they applied many rate of reaction for CO , r_{CO} , but only the rate of reaction of empirical rate expression derieved from the numerical fitting is the most accurate and simplest among all rate of equation of CO , r_{CO} [11].

It is assumed that the reactor is plug flow and isothermal [11]. Although these assumptions are not entirely correct, they allow observation of the general reactor behavior.

Figure 4.4 [11] shows for at approximately an equal molar of H_2O and CO mixture, the effect of space velocity VS conversion of CO (%). The three isotherms in this figure show that as expected the conversion of the WGS reaction decreases slowly with increasing space velocity.

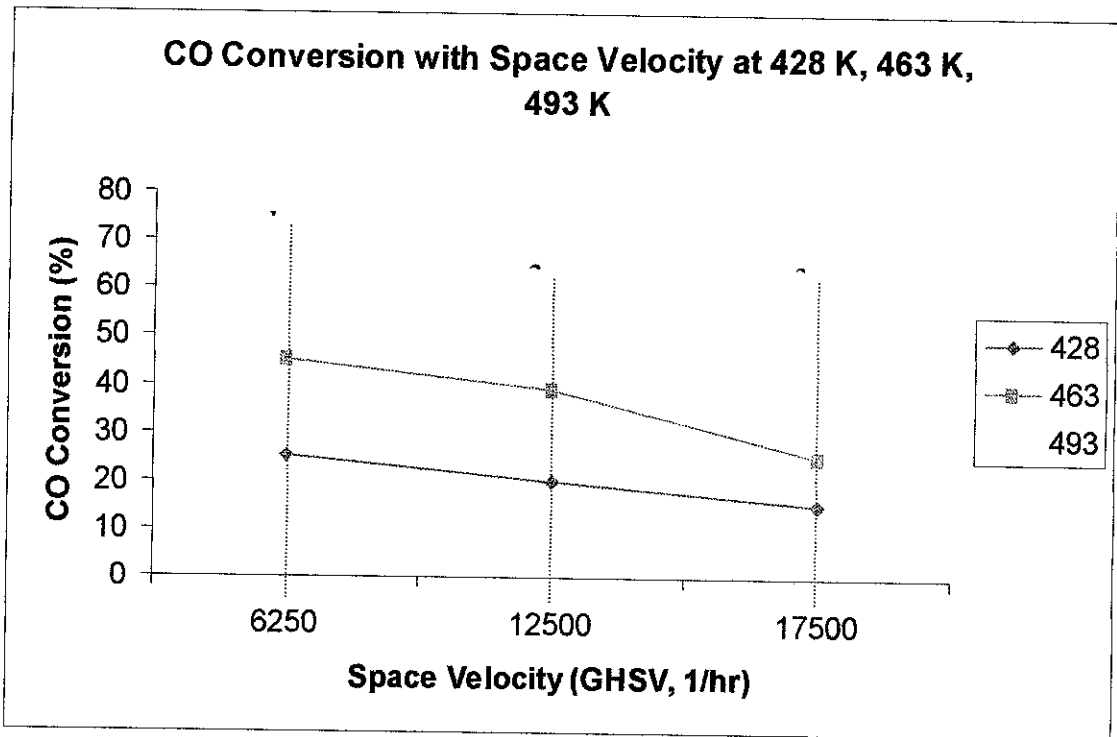


Figure 4.3: Water Gas Shift Reaction - CO conversion as a function of space velocity

To determine the predicted rate of equation, r_{CO} various slopes were taken at each of the three temperatures in order to differentiate with the measured rate of equation, r_{CO} of all three models. The slopes of each of the points were calculated manually. Based on Figure 4.4, only three points (1) 6250 hr⁻¹, (2) 12500 hr⁻¹, (3) 17500 hr⁻¹ were taken at each temperature.

For the temperature of 428 K;

$$r_A = \frac{25}{6250}$$

$$= 4 \times 10^{-3}$$

$$r_A = \frac{20}{12500}$$

$$= 1.6 \times 10^{-3}$$

$$r_A = \frac{15}{17500}$$

$$= 8.57 \times 10^{-4}$$

Thus, by doing the same method of finding the value of the slope (predicted r_{CO}) to both temperature, value of each slopes are represented in *Table 4.12*

Points Temperatures	1	2	3
428 K	4×10^{-3}	1.6×10^{-3}	8.57×10^{-4}
463 K	7.2×10^{-3}	3.12×10^{-3}	1.33×10^{-3}
493 K	0.01104	4.64×10^{-3}	2.88×10^{-3}

Table 4.12: Value of slopes (predicted r_{CO}) at temperature 428, 463, 493 K

Then, the r_{CO} is calculated by using MATLAB software by referring the equation given in the work of Choi et al. [11], which is the rate of reaction of empirical rate expression derived from the numerical fitting. The equations and variables are written in *.m format and then it is then saved by the name of **WGS-numec_fit.m**. The MATLAB language can be referred in *Appendix 7* for more details.

$$r_{CO} = 2.96 \times 10^5 e^{-E/RT} \left(P_{CO} P_{H_2O} - \frac{P_{CO_2} P_{H_2}}{K_e} \right)$$

Where

$H_2O = a$

$CO = b$

$CO_2 = c$

$H_2 = d$

The activation energy for the empirical model is 47.4 kJ/mol [11], which is consistent with other values from other literature of WGS. Equilibrium constant, K_e is calculated by referring to the equation in Choi et al. [11].

$$K_e = \exp\left(\frac{4577.8}{T} - 4.33\right)$$

Thus, by using MATLAB, the calculated r_{CO} are:

- For $T_1= 428$ K; and $K_e= 581.6$

$$r_{CO} = k \times \exp(E/(R \times T_1)) \times (P_b \times P_d) - (P_c \times P_d/K_{e1})$$

$$r_{CO} = 0.0014$$

- For $T_2= 463$ K; and $K_e= 259.11$

$$r_{CO} = k \times \exp(E/(R \times T_2)) \times (P_b \times P_d) - (P_c \times P_d/K_{e2})$$

$$r_{CO} = 0.0039$$

- For $T_3= 493$ K; and $K_e= 141.96$

$$r_{CO} = k \times \exp(E/(R \times T_3)) \times (P_b \times P_d) - (P_c \times P_d/K_{e3})$$

$$r_{CO_3} = 0.0082$$

Then, each value of r_{CO} for each temperature will be manually estimated on *Figure 4.4* by spotting the average value within the appropriate points. Let say, for the value r_{CO} of 428 K, which is 0.0014, the value is somehow located between point 2 and point 3. Thus, the conversion, X for r_{CO} of 0.0014 is estimated 24 %. The same method is applied to the rest of r_{CO} so that the conversion, X for each r_{CO} can be determined. *Table 4.13* shows the conversion, X for each average r_{CO} .

Temperature, K	r_A , mol gcat ⁻¹ h ⁻¹	Conversion, X
428	0.0014	0.24
463	0.0039	0.45
493	0.0082	0.68

Table 4.13: Conversion, X of r_{CO} for each Temperature for empirical rate expression derived from the numerical fitting

Like always, the highest temperature, which is 493 K will be selected as it is assumed as an exit temperature of the shift reactor. The conversion, X of temperature at 493 K is 0.68. According to *Figure 4.4*, at 0.68 of X , the space velocity will be approximately about 6250 h⁻¹.

Based on the journal of Rioche et al. [2], by using the equation of GHSV, the volumetric flowrate of gaseous model compound can be determined.

$$GHSV = \text{Volumetric Flow rate of Gaseous Model Compound} / \text{Volume of Catalyst}$$

In the work of Choi et al. [11], the volume of catalyst is 22.6 inch³ (360.4 cm³). Therefore, by doing the back calculation to get the volumetric flow rate of gaseous model compound after the shift reactor:

$$\begin{aligned}
& \text{Volumetric Flow rate of Gaseous Model Compound} \\
& = 6250 \text{ h}^{-1} \times 360.4 \text{ cm}^3 \\
& = 2,252,500 \text{ cm}^3 \text{ h}^{-1} \\
& = 2.2525 \text{ m}^3 \text{ h}^{-1}
\end{aligned}$$

According to the calculation above, it can be concluded that the amount of volumetric flow rate of gaseous model compound exiting the shift reactor is 2.2525-m³ h⁻¹.

4.2.2 The calculation of Component Balance

Based on the work of Huang et al. [18], the component balance of gas phase can be represented as:

$$\frac{n_{f_i} |_{z}}{\Delta z} + \frac{n_{f_i} |_{z+\Delta z}}{\Delta z} - \frac{\pi d \Delta z J}{\Delta z} + \frac{1}{4 \Delta z} \pi d^2 \Delta z r_i = 0$$

Simplify and integrate

$$n_{si} = \frac{1}{4} \pi d_{in}^2 J(z) - \pi d_{in} J(z) + c$$

Based on the Huang et al. [18], the $n_{i,f}$ for each component are:

$$n_{CO,g} = 6.35 \times 10^{-3} \text{ mol s}^{-1}$$

$$n_{H_2O,g} = 0.11557 \text{ mol s}^{-1}$$

$$n_{H_2,g} = 0.4134 \text{ mol s}^{-1}$$

$$n_{CO_2,g} = 0.09843 \text{ mol s}^{-1}$$

$$n_{N_2,g} = 0$$

$$n_{CH_4,g} = 1.27 \times 10^{-3} \text{ mol s}^{-1}$$

And

$$J = 152400 \text{ mol/cm}^2/\text{s}$$

$$d_{in} = 0.1 \text{ cm}$$

B.C. at $z=L$

$$n_{CO,g} = 0$$

$$n_{H_2O,g} = 0$$

$$n_{H_2,g} = 5 \times 10^{-7} (n_{i,0}) = 3.175 \times 10^{-7} \text{ mol s}^{-1}$$

$$n_{CO_2,g} = 370 \times 10^{-6} (n_{i,0}) = 2.3495 \times 10^{-4} \text{ mol s}^{-1}$$

Apply B.C. in order to determine the constant, c for each component

For CO

$$c = -\frac{1}{4}\pi(0.1)^2(152400)(L) + \pi(0.1)(152400)(L)$$

For H_2O

$$c = -\frac{1}{4}\pi(0.1)^2(152400)(L) + \pi(0.1)(152400)(L)$$

For H_2

$$c = -\frac{1}{4}\pi(0.1)^2(152400)(L) + \pi(0.1)(152400)(L) + 3.175 \times 10^{-7}$$

For CO_2

$$c = -\frac{1}{4}\pi(0.1)^2(152400)(L) + \pi(0.1)(152400)(L) + 2.3495 \times 10^{-4}$$

The product produced in the shift reactor contains only H_2 and CO_2 components. Thus, two components such as CO and H_2O are not contained in the product stream. ($z = 61$ cm)

For CO

$$n_{CO,s} = 0$$

For H_2O

$$n_{H_2O,s} = 0$$

For H_2

$n_{H_2,s}$

$$= \frac{1}{4} \pi (0.1)^2 (152400)(61) - \pi (0.1)(152400)(61) + \pi (0.1)(152400)(61) - \frac{1}{4} \pi (0.1)^2 (152400)(61) + 3.175 \times 10^{-7}$$

$$= 3.175 \times 10^{-7} \text{ mol s}^{-1}$$

For CO_2

$n_{CO_2,s}$

$$= \frac{1}{4} \pi (0.1)^2 (152400)(61) - \pi (0.1)(152400)(61) + \pi (0.1)(152400)(61) - \frac{1}{4} \pi (0.1)^2 (152400)(61) + 2.3495 \times 10^{-4}$$

$$= 2.3495 \times 10^{-4} \text{ mol s}^{-1}$$

4.3 Hydrogen Purification (PSA Purification)

4.3.1 The calculation of Component Balance

For the PSA column, literature of Ribeiro et al. [12] is used to model the hydrogen purification system. Basically, the system from this literature used activated carbon as a bed for the column with the length of 0.5 m. Based on the work of Ribeiro et al. [12], the component balance of gas phase can be represented as:

$$\frac{d}{dz} \left(\varepsilon D_{ax} n_{g,i} \frac{dy_i}{dz} \right) - \frac{d}{dz} (u_0 n_{i,g}) - \varepsilon \frac{dn_{g,i}}{dt} - \frac{(1-\varepsilon) a_p k_f}{1 + Bi_i} (n_{g,i} - \bar{n}_{p,i}) = 0$$

At B.C. 1 which is $z = 0$

$$u_0, n_{in,i} = u_0 n_{i,g} - \varepsilon D_{ax} n_{g,i} \frac{dy_i}{dz}$$

Then replace the B.C.1 into the above equation. The new equation of component balance will be:

$$-\frac{d}{dz}(u_0, n_{in,i}) - \varepsilon \frac{dn_{g,i}}{dt} - \frac{(1-\varepsilon)(a_p)(k_f)}{1+Bi_j}(n_{g,i}) = 0$$

$$k_f = 9.28 \times 10^{-2} \text{ ms}^{-1}$$

$$u_0 = 0.46 \text{ ms}^{-1}$$

$$a_p = \frac{A}{V}$$

$$= \frac{1.72 \times 10^{-5}}{6.7 \times 10^{-9}}$$

$$= 2567.4 \text{ m}^{-1}$$

$$R_p = 1.17 \times 10^{-3} \text{ m}$$

$$\varepsilon_p = 0.566$$

$$\Omega_M = 3/5$$

$$D_{p,H_2} = 4.99 \times 10^{-6} \text{ m}^2/\text{s}$$

$$D_{p,CO_2} = 279.99 \text{ m}^2/\text{s}$$

Thus, use the new equation in order to determine $n_{g,i}$:-

For H_2

$$-\frac{d}{dz}(0.46 \times 3.175 \times 10^{-7}) - 0.38 \frac{dn_{g,H_2}}{dt} - \frac{(1-0.38)(2567.4)(9.28 \times 10^{-2})}{1+192.46}(n_{g,H_2}) = 0$$

$$n_{f,CO_2} = 3.175 \times 10^{-7} \text{ mol s}^{-1}$$

$$Bi_{H_2} = \frac{a_p k_f R_p^2}{\varepsilon_p \Omega_M D_{p,H_2}}$$

$$= \frac{2567.4(0.0928)(1.17 \times 10^{-3})^2}{(0.566)(3/5)(4.99 \times 10^{-6})}$$

$$= 192.46 \text{ (dimensionless)}$$

Integrate and solve

$$1.4605 \times 10^{-7} (t) = 0.38(n_{g,H_2})(z) + 0.765(n_{g,H_2})$$

At $t = 80,000$ s (500 cycle number) as stated in literature of Ribeiro et al. [12] (to obtain the maximum purity of H_2) and $z = 0.5$ m, thus

$$n_{g,H_2} = 0.01 \text{ mol s}^{-1}$$

For CO_2

$$-\frac{d}{dz} (0.46 \times 2.3495 \times 10^{-4}) - 0.38 \frac{dn_{g,CO_2}}{dt} - \frac{(1-0.38)(2567.4)(9.28 \times 10^{-2})}{1+279.99} (n_{g,CO_2}) = 0$$

$$n_{f,CO_2} = 2.3495 \times 10^{-4} \text{ mol s}^{-1}$$

$$Bi_{CO_2} = \frac{2567.4(0.0928)(1.17 \times 10^{-3})^2}{(0.566)(3/5)(3.43 \times 10^{-6})}$$

$$= 279.99 \text{ (dimensionless)}$$

Integrate and solve

$$1.08 \times 10^{-4} (t) = 0.38(n_{g,CO_2})(z) + 0.765(n_{g,CO_2})$$

At $t = 80,000$ s and $z = 0.5$ m, thus

$$n_{g,CO_2} = 9.05 \text{ mol s}^{-1}$$

Since only H_2 and CO_2 that are produced from the shift reactor, these two will be the only products that will flow at the outlet of PSA column stream. *Table 4.12* shows the calculated molar flowrates along the bed of activated carbon from 0 m to 0.5 m at 80,000 s in order to compare the purity of hydrogen of this project with the work of Ribeiro et al. [12]. *Figure 4.5* and *Figure 4.6* show the trends of the molar flowrate for both H_2 and CO_2 along the bed.

Length (m)	Molar flowrate of H_2 (mol s^{-1})	Molar flowrate of CO_2 (mol s^{-1})
0.0	0.02	11.29
0.1	0.01	10.76
0.2	0.01	10.27
0.3	0.01	9.83
0.4	0.01	9.42
0.5	0.01	9.05

Table 4.14: Calculated molar flowrates for H_2 and CO_2 along the bed from 0 m to 0.5 m at $t=80,000$ s

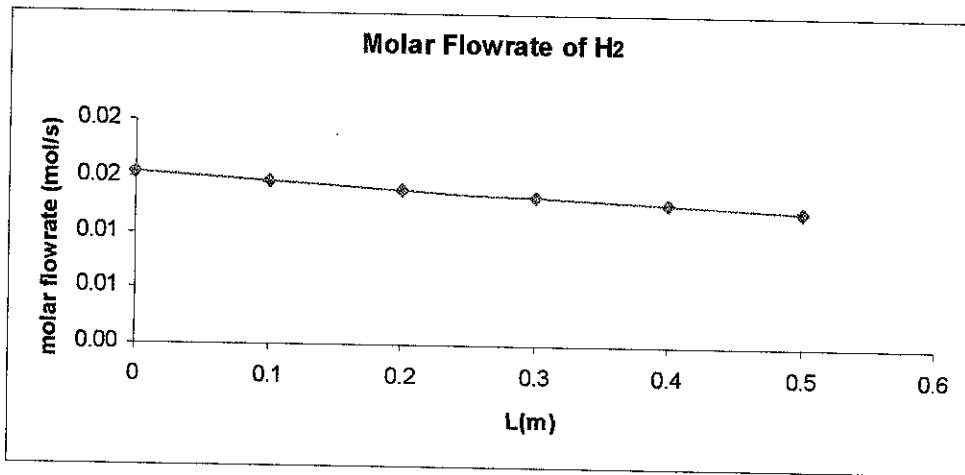


Figure 4.4: Graph of molar flowrate for H_2 along the bed from 0 m to 0.5 m at 80,000 s

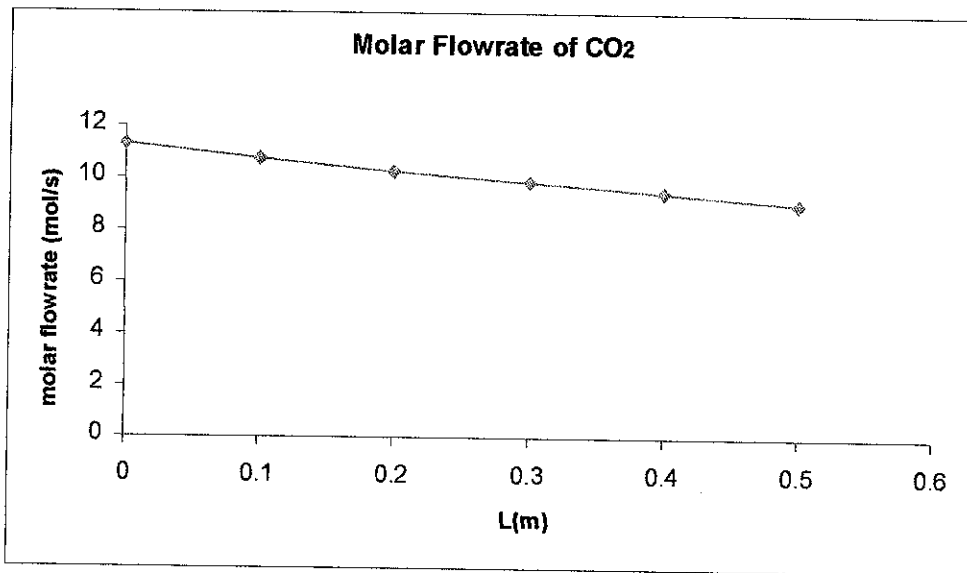


Figure 4.5: Graph of molar flowrate for CO₂ along the bed from 0 m to 0.5 m at 80,000 s

According to these two graphs, it is concluded that the amount of molar flowrates for both H₂ and CO₂ are decreasing with the increasing length of activated carbon bed (z). This is because the high diffusivity value makes both the uptake and regeneration more difficult, which broadens the H₂ and CO₂ along the bed. Although the molar flowrate of H₂ seems to be decreasing with the increasing length of bed, it is clear that somehow the flowrate will stay constant.

According to the work of Ribeiro et al. [12], the amount of cycle number is more than 500 cycle number (>80,000 s). This is because with the longer the period, the whole bed can achieved the stabilization of temperature, thus make the purification process better. This process also shows that the CO₂ does stay in the activated carbon area, which satisfy the design requisite of this process.

According to the work of Rioche et al. [15], the formula of H₂ purity can be represented as

$$H_2 \text{ purity \%} = \frac{\text{moles of H}_2 \text{ obtained (at } z = 0.5 \text{ m at } t = 80,000\text{s)}}{(2n + m/2 - k) \times \text{moles of carbon in the feed}}$$

The feed is ethanol, which C_2H_6O . Thus, that makes $n=2$, $m=6$, and $k=1$. And also amount of moles of carbon in the feed is 1.685×10^{-3} .

$$\begin{aligned} H_2 \text{ purity } \% &= \frac{0.01}{(2(2) + 6/2 - 1) \times 1.685 \times 10^{-3}} \times 100 \\ &= 98.9119 \% \end{aligned}$$

The amount of H_2 purity for this work is 98.9119 %, less than the amount of H_2 purity of Ribeiro et al. [12], which is 99.9994 % although the cycle number is the same (500 cycles or 80,000 s). The reason is the work of Ribeiro et al. [12] used double layer beds consisting of both activated carbon and zeolite. This will make the purification process more effective and efficient. Whereas for this work, the bed only consist of activated carbon with the purpose is to trap the carbon dioxide. Thus, by comparing this work and Ribeiro et al. [12], the relative error (%) can be determined.

$$\begin{aligned} \text{Relative error } \% &= \left| \frac{98.9119 - 99.9994}{99.9994} \right| \times 100 \\ &= 1.08 \% \end{aligned}$$

CHAPTER 5: CONCLUSION

Basically, in conclusion of this project, the objectives of this project are achieved. But, there is a weakness for this project. Supposedly, this project should use bio oil as the main sample of modeling, but due to some difficulties, the bio oil was represented by ethanol, which will replicate the kinetic modeling of bio oil. By doing this project, the aim to develop the modeling way to simulate the sequence of processes in hydrogen production from bio-oil in MATLAB can be achieved significantly.

Based on the results of kinetic modeling of steam reforming, Model 1 does not yield a satisfaction result, as the Average Relative Error is high, which is 29.1%. For Model 2 and Power Law, both have the Average Relative Error of 21.1% and 17.2% respectively. Based on Akande et al. [10], if the Average Relative Error is less than 25 %, then it can be considered as a good result. Basically, Model 2 and Power Law are on the active site of the Rate Determining Step as the Average Relative Error is less than 25 %.

For the Water Gas Shift reaction, it is concluded that the final temperature for the shift reactor for this system is around 493 K. The conversion of the reactor at the temperature of 493 K is 68 % and thus, the GHSV will be approximately about 6250 h^{-1} . According to Choi et al. [11] the rate of reaction of empirical rate expression derived from the numerical fitting is the most accurate and simplest among all rate of equation of CO . Based on the molar balance calculation, only two products produced in the shift reactor, which are H_2 and CO_2 as they will be sent to PSA column.

For the PSA purification of hydrogen, H_2 and CO_2 will be the only products that will flow at the outlet of PSA column stream. Based on the results, the amount of molar flowrates for both H_2 and CO_2 are decreasing with the increasing length of activated carbon bed (z). The H_2 purity for this work is 98.9119 % because the bed only consists of activated carbon with the purpose is to trap CO_2 . It is determined that the Relative error (%) for this work and Ribeiro et al., based on H_2 purity is 1.08 %.

REFERENCES

- [1] Abedi J, Yeboah YD, Realff M, McGee D, Howard J, Bota KB. An integrated approach to hydrogen production from agricultural residues for use in urban transportation. In: Proceedings of the 2001 DOE hydrogen program review NREL/ CP-570-30535.
- [2] Rioch CE, Kulkarni S, Meunier FC, Breen JP, Burch R. Steam reforming of model compounds and fast pyrolysis bio-oil on supported noble metal catalysts. *Appl Catal B Environ* 2005;61:130–9.
- [3] Huber GW, Dumesic JA. An overview of aqueous-phase catalytic processes for production of hydrogen and alkanes in a biorefinery. *Catal Today* 2006;111(1–2):119–32.
- [4] Piskorz J, Scott DS, Radlein D. In: Soltes EJ, Milne TA., editors. Pyrolysis oils from biomass: producing, analyzing and upgrading. ACS Symposium Series 376. Washington, DC: American Chemical Society; 1988. p. 167–78.
- [5] Chernik S, Wang D, Montane D, Chornet E. In: Bridgwater AV, Boocock DGB., editors. Developments in thermochemical biomass conversion. London: Blackie Academic & Professional; 1996. p. 672–86.
- [6] Garcia L, French R, Czernik S, Chornet E. Catalytic steam reforming of bio-oils for the production of hydrogen: effects of catalyst composition. *Appl Catal A General* 2000;201:225–39.
- [7] Diebold J, Scahill J. In: Soltes EJ, Milne TA., editors. Pyrolysis oil from biomass. ACS Symposium Series 376. Washington, DC: American Chemical Society. 1998. p. 31.
- [8] Evans RJ, Milne TA. Molecular characterization of the pyrolysis of biomass. 1 Fundamental. *Energy Fuels* 1987; 1(2):123.
- [9] Douglas J.M., *Conceptual Design of Chemical Process*, New York, McGraw Hill Chemical Engineering Series, 1998.
- [10] Kinetic Modeling of Hydrogen production by the catalytic reforming of crude ethanol over a co-precipitated Ni-Al₂O₃ catalyst in a packed bed tubular reactor. - Abayomi Akande, Ahmed Aboudheir, Raphael Idem, Ajay Dalai.

- [11] “Water gas shift reaction kinetics and reactor modeling for fuel cell grade hydrogen”- Yongtaek Choi, Harvey G. Stenger -Department of Chemical Engineering, Lehigh University, Bethlehem, PA 18015, USA
- [12] “A parametric study of layered bed PSA for hydrogen purification” - Ana M. Ribeiro, Carlos A. Grande, Filipe V.S. Lopes, José M. Loureiro, Alírio E. Rodrigues Laboratory of Separation and Reaction Engineering (LSRE), Associate Laboratory, Department of Chemical Engineering, Faculty of Engineering, University of Porto, Rua Dr. Roberto Frias, s/n, 4200-465 Porto, Portugal
- [13] Vagia, CE and Lemonidou, A.A. “Thermodynamic analysis of hydrogen production via steam reforming of selected components of aqueous bio-oil fraction”, *International Journal of Energy*, 33,212-223,2007.
- [14] “Thermodynamic analysis of hydrogen production via steam reforming of selected components of aqueous bio-oil fraction” - Ekaterini Ch. Vagia, Angeliki A. Lemonidou - Department of Chemical Engineering, Aristotle University of Thessaloniki and CERTH/CPERI, P.O. Box 1517, University Campus, GR-54006 Thessaloniki, Greece.
- [15] Cyrille Rioche, Shrikant Kulkarni, Frederic C. Meunier , John P. Breen, Robbie Burch CenTACat, Queen’s University Belfast, Belfast, BT9 5AG Northern Ireland, UK (2005).
- [16] “Simulation of Pyrolysis Bio-oil Upgrading Into Hydrogen” – Murni M. Ahmad, Laveena M. Chugani, Cheng Seong Khor and Suzana Yusup – Chemical Engineering Department, Universiti Teknologi Petronas, Perak, Malaysia.
- [17] “Hydrogen from biomass-production by steam reforming of biomass pyrolysis oil” - Stefan Czernik, Robert Evans, Richard French - National Renewable Energy Laboratory, 1617 Cole Boulevard, Golden, CO 80401, United States
- [18] “Modeling of CO₂-selective water gas shift membrane reactor for fuel cell’ - Jin Huang, Louei El-Azzami, and W.S. Winston Ho. Department of Chemical and Biomolecular Engineering, The Ohio State University, 2041 College Road, Columbus, OH 43210-1180, USA.
- [19] M.-C. Yang, E.L. Cussler, Designing hollow-fiber contactors, *AIChE J.* 32 (1986) 1910–1916.

- [20] Pure hydrogen from pyrolysis oil using the steam-iron process - M.F. Bleeker, S.R.A. Kersten, H.J. Veringa. University of Twente, Department of Science and Technology, Enschede, The Netherlands
- [21] Mathematical modelling of low-temperature hydrogen production with in situ CO₂ capture - Georgios C. Koumpouras, Esat Alpay, Frantisek Stepanek
- [22] Ethanol steam reforming in a dense Pd-Ag membrane reactor: A modeling work. Comparison with the traditional system – F Gallucci, M De Falco, S Tosti, L Marrelli, A Basile.

APPENDICES

Appendix 1: Operating Unit Description

Mixer

The feed (bio and water) entering the process are mixed before heated up in a furnace.

Furnace

The stream from the mixer is heated up from 41°C to 650°C using a furnace due to the need of high temperature requirement before it is fed to the steam reformer.

Steam Reformer

The stream from the furnace is fed to fixed bed catalytic reformer that operates at 650°C and 1 bar. The reforming of the bio oil will produce CH_4 , CO_2 , H_2 , and CO .

Shift Reactor

The stream is cooled to 200°C and compressed to 17.5 bar before entering the shift reactor. The hydrogen yield is maximized by shift conversion where carbon monoxide reacts with steam to produce carbon monoxide.

Flash Drum

The gaseous mixture, which is rich in hydrogen content, is cooled to 30°C before it is separated in flash drum at 16 bar. The steam is condensed to water, which is separated from the gaseous mixture.

Pressure Swing Absorption (PSA)

The gaseous mixture is purified into hydrogen rich gas stream in PSA. The driving force for the separation is the difference in impurity partial pressure between the feed and the tail gas. The feed pressure range is between 15 to 29 bar. The tail gas pressure is chosen to be as low as possible for the pressure, which is normally around 1 to 2 bar. The operating temperature for PSA is 35°C.

Coolers

For the 1st cooler, it is used to cool the hot stream from steam reformer from 500°C to 200°C before entering the shift reactor, which operates lower than 200°C. The 2nd cooler is used to cool the hot stream from the shift reactor 200°C to 30°C before entering the flash drum. The cooling medium is Molten salt for both of these coolers.

Appendix 4: steam_reforming_model1.m

```
%MODEL 1
%1st temp=593 for 1st trial
r11=[k*exp(-E/(R*T1))]*[Na11-
(Nc11^2*Nd11^6)/(Kp1*Nb11^3)]/[1+((Kf*Nc11*Nd11^3)/(Nb11))+((Kg*Nc11*Nd
11^3)/(Nb11^2))+((Ke*Nc11^2*Nd11^6)/(Nb11^3)))]
k=8.91E+002;
E=4.03E+003;
R=8.314;
T1=593;
Na11=5.70596E-009;
Nb11=1.57331E-007;
Nc11=8.40614E-009;
Nd11=2.40685E-008;
Kp1=2.45431E+011;
Kf=0.0;
Kg=0.0;
Ke=0.0;

%1st temp=593 for 2nd trial
r12=[k*exp(-E/(R*T1))]*[Na12-
(Nc12^2*Nd12^6)/(Kp1*Nb12^3)]/[1+((Kf*Nc12*Nd12^3)/(Nb12))+((Kg*Nc12*Nd
12^3)/(Nb12^2))+((Ke*Nc12^2*Nd12^6)/(Nb12^3)))]
Na12=8.43861E-009;
Nb12=2.0793E-007;
Nc12=8.811424E-009;
Nd12=2.52289E-008;

%1st temp=593 for 3rd trial
r13=[k*exp(-E/(R*T1))]*[Na13-
(Nc13^2*Nd13^6)/(Kp1*Nb13^3)]/[1+((Kf*Nc13*Nd13^3)/(Nb13))+((Kg*Nc13*Nd
13^3)/(Nb13^2))+((Ke*Nc13^2*Nd13^6)/(Nb13^3)))]
Na13=1.64558E-008;
Nb13=3.51408E-007;
Nc13=9.27356E-009;
Nd13=2.65521E-008;

%2nd temp=693 for 1st trial
r21=[k*exp(-E/(R*T2))]*[Na21-
(Nc21^2*Nd21^6)/(Kp2*Nb21^3)]/[1+((Kf*Nc21*Nd21^3)/(Nb21))+((Kg*Nc21*Nd
21^3)/(Nb21^2))+((Ke*Nc21^2*Nd21^6)/(Nb21^3)))]
T2=693;
Na21=5.02195E-009;
Nb21=1.57821E-007;
Nc21=1.0229E-008;
Nd21=2.92878E-008;
Kp2=3.36674E+015;

%2nd temp=693 for 2nd trial
r22=[k*exp(-E/(R*T2))]*[Na22-
(Nc22^2*Nd22^6)/(Kp2*Nb22^3)]/[1+((Kf*Nc22*Nd22^3)/(Nb22))+((Kg*Nc22*Nd
22^3)/(Nb22^2))+((Ke*Nc22^2*Nd22^6)/(Nb22^3)))]
Na22=9.80704E-009;
Nb22=2.41648E-007;
```

Nc22=1.02403E-008;
Nd22=2.93201E-008;

%2nd temp=693 for 3rd trial

r23=[k*exp(-E/(R*T2))]*[Na23-
(Nc23^2*Nd23^6)/(Kp2*Nb23^3)]/[1+((Kf*Nc23*Nd23^3)/(Nb23))+((Kg*Nc23*Nd
23^3)/(Nb23^2))+((Ke*Nc23^2*Nd23^6)/(Nb23^3))]
Na23=1.73306E-008;
Nb23=3.66116E-007;
Nc23=9.18524E-009;
Nd23=2.62993E-008;

%3rd temp=793 for 1st trial

r31=[k*exp(-E/(R*T3))]*[Na31-
(Nc31^2*Nd31^6)/(Kp3*Nb31^3)]/[1+((Kf*Nc31*Nd31^3)/(Nb31))+((Kg*Nc31*Nd
31^3)/(Nb31^2))+((Ke*Nc31^2*Nd31^6)/(Nb31^3))]
T3=693;
Na31=5.11495E-009;
Nb31=1.60744E-007;
Nc31=1.04184E-008;
Nd31=2.98302E-008;
Kp3=4.45742E+018;

%3rd temp=793 for 2nd trial

r32=[k*exp(-E/(R*T3))]*[Na32-
(Nc32^2*Nd32^6)/(Kp3*Nb32^3)]/[1+((Kf*Nc32*Nd32^3)/(Nb32))+((Kg*Nc32*Nd
32^3)/(Nb32^2))+((Ke*Nc32^2*Nd32^6)/(Nb32^3))]
Na32=8.52993E-009;
Nb32=2.21894E-007;
Nc32=1.06204E-008;
Nd32=3.04085E-008;

%3rd temp=793 for 3rd trial

r33=[k*exp(-E/(R*T3))]*[Na33-
(Nc33^2*Nd33^6)/(Kp3*Nb33^3)]/[1+((Kf*Nc33*Nd33^3)/(Nb33))+((Kg*Nc33*Nd
33^3)/(Nb33^2))+((Ke*Nc33^2*Nd33^6)/(Nb33^3))]
Na33=1.62475E-008;
Nb33=3.50781E-007;
Nc33=9.71516E-009;
Nd33=2.78165E-008;

```
Nc23=9.18524E-009;  
Nd23=2.62993E-008;
```

```
%3rd temp=793 for 1st trial
```

```
r31=[k*exp(-E/(R*T3))]*[Na31-  
(Nc31^2*Nd31^6)/(Kp3*Nb31^3)]/[1+(Ka*Na31)]^2  
T3=693;  
Na31=5.11495E-009;  
Nb31=1.60744E-007;  
Nc31=1.04184E-008;  
Nd31=2.98302E-008;  
Kp3=4.45742E+018;
```

```
%3rd temp=793 for 2nd trial
```

```
r32=[k*exp(-E/(R*T3))]*[Na32-  
(Nc32^2*Nd32^6)/(Kp3*Nb32^3)]/[1+(Ka*Na32)]^2  
Na32=8.52993E-009;  
Nb32=2.21894E-007;  
Nc32=1.06204E-008;  
Nd32=3.04085E-008;
```

```
%3rd temp=793 for 3rd trial
```

```
r33=[k*exp(-E/(R*T3))]*[Na33-  
(Nc33^2*Nd33^6)/(Kp3*Nb33^3)]/[1+(Ka*Na33)]^2  
Na33=1.62475E-008;  
Nb33=3.50781E-007;  
Nc33=9.71516E-009;  
Nd33=2.78165E-008;
```

Appendix 6: power_law_model.m

```
*POWER LAW MODEL
%1st temp=593 for 1st trial
r11=[k*exp(-E/(R*T1))]*[Na11]^0.43
k=3.12E-002;
E=4.41E+003;
R=8.314;
T1=593;
Na11=5.70596E-009;

%1st temp=593 for 2nd trial
r12=[k*exp(-E/(R*T1))]*[Na12]^0.43
Na12=8.43861E-009;

%1st temp=593 for 3rd trial
r13=[k*exp(-E/(R*T1))]*[Na13]^0.43
Na13=1.64558E-008;

%2nd temp=693 for 1st trial
r21=[k*exp(-E/(R*T2))]*[Na21]^0.43
T2=693;
Na21=5.02195E-009;

%2nd temp=693 for 2nd trial
r22=[k*exp(-E/(R*T2))]*[Na22]^0.43
Na22=9.80704E-009;

%2nd temp=693 for 3rd trial
r23=[k*exp(-E/(R*T2))]*[Na23]^0.43
Na23=1.73306E-008;

%3rd temp=793 for 1st trial
r31=[k*exp(-E/(R*T3))]*[Na31]^0.43
T3=693;
Na31=5.11495E-009;

%3rd temp=793 for 2nd trial
r32=[k*exp(-E/(R*T3))]*[Na32]^0.43
Na32=8.52993E-009;

%3rd temp=793 for 3rd trial
r33=[k*exp(-E/(R*T3))]*[Na33]^0.43
Na33=1.62475E-008;
```

Appendix 7: WGS-numec_fit.m

```
% According to Yongtaek Choi and Harvey G. Stenger [11], they used an
empirical
% expression derived from the numerical fitting. The reason is because
of
% its accuracy and simplicity.

% The components will be represented with the alphabets for easy
reference
% H2O = a
% CO = b
% CO2 = c
% H2 = d

% For 1st temperature, T= 428 K
% The parameters that will be involved:
k= 2.96E+005;
Pa= 0.58;
Pb= 0.005;
Pc= 0.015;
Pd= 0.4;
E= -47.4E+003;
R= 8.314;
T1= 428;
Ke1= 581.6;
% The rate expression of numerical fitting:
rCO1=k*exp(E/(R*T1))*(Pb*Pa)-(Pc*Pd/Ke1)

% For 2nd temperature, T= 463 K
% The parameters that will be involved:
T2= 463;
Ke2= 259.11;
% The rate expression of numerical fitting:
rCO2=k*exp(E/(R*T2))*(Pb*Pa)-(Pc*Pd/Ke2)

% For 3rd temperature, T= 493 K
% The parameters that will be involved:
T3= 493;
Ke3= 141.96;
% The rate expression of numerical fitting:
rCO3=k*exp(E/(R*T3))*(Pb*Pa)-(Pc*Pd/Ke3)
```